



Latency, Bandwidth, and Control Loop Residual Relationships

Keck Adaptive Optics Note 710

Donald Gavel, UCSC

Feb. 12, 2010

■ Abstract

This is a description of how latency in a [open | closed] loop controller maps to wavefront rms error

■ Introduction

The Taylor frozen-flow atmosphere has the power spectrum¹

$$S_{\phi}[f] := 0.0770491 (r_0 / v)^{-5/3} f^{-8/3} \quad (1)$$

radians²/Hz. To convert to nanometers²/Hz, multiply by $(\lambda/2\pi)^2$. A control law simply acts as a transfer function, $H_C[f]$, on the spectrum of wavefront disturbance. This function is designed to reduce the total power in the final residual but is constrained to obey laws of causality and, in the case of closed loop control, results in a stable system. The power spectrum of the residual is

$$\ln[2]= \|\mathbf{x}_-\| := \mathbf{Abs}[\mathbf{x}]$$

$$S_e[f] := \|H_C[f]\|^2 S_{\phi}[f] \quad (2)$$

For open-loop control, the filtering process consists of subtracting an estimated version of the wavefront from the current wavefront. The estimate is formed after integrating the wavefront sensor for a cycle time, then waiting one frame cycle for the WFS camera readout and then a compute delay to calculate the estimate. Finally the estimated wavefront is held on the actuators of the DM for one cycle time. There is no feedback.

In the Fourier domain, the open loop control process is described by

OLTF

$$H_{OLC}[f] = 1 - \left(\frac{1 - e^{-i2\pi fT}}{-i2\pi fT} \right) e^{-i2\pi f(T+\tau_c)} \left(\frac{1 - e^{-i2\pi fT}}{-i2\pi fT} \right) \quad (3)$$

where T is the sample time and τ_c is the compute delay.

A closed-loop controller has a feedback loop. Assuming integral feedback with a gain, γ , the transfer function is

CLTF

$$H_{CLC}[f] = \frac{1}{1 + \frac{\gamma}{1 - e^{-i2\pi fT}} \left(\frac{1 - e^{-i2\pi fT}}{-i2\pi fT} \right) e^{-i2\pi f(T+\tau_c)} \left(\frac{1 - e^{-i2\pi fT}}{-i2\pi fT} \right)} \quad (4)$$

The residual wavefront variance is determined by integrating $S_e[f]$ up to the Nyquist frequency :

$$\sigma_{\text{BW}}^2 = 2 \int_0^{\frac{1}{2T}} S_e[f] df \quad (5)$$

This ignores spectral contributions beyond Nyquist, which we'll categorize as "aliasing error" rather than bandwidth error. This reasonable to do for two reasons: a) the sampling time is usually chosen by design so that out-of-band contributions are negligible, b) the Hartmann subapertures actually impose a low-pass filter on the disturbance entering the controller, at a cutoff of v/d Hz where v is the wind velocity and d is the subaperture size, and, again, the sampling frequency $1/T$ is by design chosen much larger than v/d . In essence, this is saying that aliasing error due to the finite subaperture size has already counted in all the aliasing, and we don't have to re-count it in the bandwidth error calculation.

Through a change of variables, it is possible to factor out the relevant scale factors and do the integration numerically:

$$\sigma_{\text{BW}}^2 = (v T / r_0)^{5/3} \zeta \quad (6)$$

where ζ is a constant that depends on the case of open or closed loop, the delay parameter $\alpha = \tau_c/T$, and in the case of closed loop, the closed loop gain, γ .

■ Comparison to a Greenwood Frequency model

The Greenwood Frequency is a parameter relating the rms closed loop residual in an ideal continuous-time integral feedback controller to the atmospheric conditions and the closed-loop -3db rejection frequency, f_c . From Greenwood, formula (9.53):

$$\sigma_{\text{BW}}^2 = (f_g / f_c)^{5/3} \quad (7)$$

On the other hand, the parameter τ_0 relates the atmospheric conditions directly to the wind velocity. Applying equations (3.1-49) and (3.1-48) from KAON 208² we get its relation to f_g . This allows people to use f_g also as a direct measure of the atmosphere conditions without reference to a particular controller:

$$f_g = 0.135 / \tau_0 = \frac{0.135}{0.314} \times \frac{v}{r_0} \quad (8)$$

eqn9

$$\sigma_{\text{BW}}^2 = \left(\frac{0.135}{0.314} \right)^{5/3} \left(\frac{1}{f_c T} \right)^{5/3} \left(\frac{v T}{r_0} \right)^{5/3} = \zeta_g \left(\frac{v T}{r_0} \right)^{5/3} \quad (9)$$

The definition of f_c however is rather unclear. Discrete time control systems do not act as simply as continuous time systems because of system delays inherent with exposure time, readout, and computation. It is difficult to get a rejection bandwidth (-3db point) that is more than about 1/10 of the sample frequency, and also difficult to create a rejection function that doesn't overshoot (go above 1) at higher frequencies. The rejection curves in the Appendix show that, with a compute delay combined with the camera readout, WFS integration, and DM hold times, the bandwidth is about $0.05/T$ when the compute delay is one sample and $0.025/T$ when the compute delay is two samples. Substituting this in to (9) gives approximate values for ζ_g :

$$\zeta_g = \left(\frac{0.135}{0.314} \right)^{5/3} \left(\frac{1}{f_c T} \right)^{5/3} / . f_c \rightarrow \left\{ \frac{0.05}{T}, \frac{0.025}{T} \right\} \quad (10)$$

{36.0903, 114.579}

■ Comparison to a pure time-lag (τ_0) model

In a simple open-loop lag model, the correction is applied τ_d seconds delayed. The residual is then

$$\sigma_{BW}^2 = 6.88 \left(\frac{v \tau_d}{r_0} \right)^{5/3} = \zeta_0 \left(\frac{v T}{r_0} \right)^{5/3} \tag{11}$$

We can approximate the WFS stare time and DM hold time as latency delays of 1/2 a sample period each. The approximation is justified by noting that this is the "average" age of the data in each case (the calculations in the next section vindicate this). Add to this WFS readout time and compute delays of either one or two sample periods and the equivalent values for ζ_0 are:

$$\zeta_0 = 6.88 \left(\frac{\tau_d}{T} \right)^{5/3} \quad / . \tau_d \rightarrow \{3 T, 4 T\} \tag{12}$$

{42.9329, 69.3461}

■ **Discrete time systems**

In the Appendix we show that the actual values of ζ for the discrete transfer function (DTF) are considerably larger than the model approximations ζ_g and ζ_0 , owing to the fact that the delays actually cause overshoot (gains > 1 at some high frequency band) in the rejection curves. For open-loop the values are: $\zeta = 84$ and 137 for one and two T compute delays respectively. For closed-loop (with optimally tuned feedback gain) the values are: $\zeta = 98$ and 172 for one and two T compute delays respectively.

	$\tau_c = T$	$\tau_c = 2 T$
Greenwood model (f_g)	36	115
Time lag model (τ_0)	43	69
Closed loop DTF	98	172
Open loop DTF	84	137

Table 1 Normalized residual variances, ζ , as computed by various methods for one and two samples of compute delay.

We can substitute the Keck NGAO nominal values for v and r_0 to translate these normalized residuals into nanometers of wavefront error. For the nominal NGAO design conditions, $v = 9$ m/sec, $r_0 = 16$ cm at $\lambda = 0.5 \mu\text{m}$ and zenith angle of 30 degrees, and $T = 0.5$ ms this yields

In[181]:= **Table2**

$\sigma_{BW}(\text{nm})$	$\tau_c=T$	$\tau_c=2T$
Greenwood model	24	44
Time-lag model	27	34
Closed loop DTF	40	53
Open Loop DTF	37	48

Out[181]=

Table 2 Residual wavefront errors for the NGAO nominal conditions $v = 9$ m/sec, $r_0 = 16$ cm at $\lambda = 0.5 \mu\text{m}$ and zenith angle of 30 degrees, and $T = 0.5$ ms. Units are nanometers, rms.

■ **Keck NGAO parameter study**

The control loop residual was calculated for the following cases relevant to NGAO³

- Compute time delays of 0, 1/2, 1, and 2 samples
- Sample rates of 2.0 kHz and 800 Hz ($T = 0.5$ milliseconds and 1.25 milliseconds)
- Wind speed of 9 m/sec and 19 m/sec
- Zenith angle of 30 degrees ($r_0 = 16$ cm)

In[117]:= $r_0 = 0.16$

For open-loop control, we use

$$\ln[123]:= \sigma[v_-, T_-, \alpha_-] := \left(\frac{500}{2\pi}\right) \sqrt{\zeta[\alpha] \left(\frac{v T}{r_0}\right)^{5/3}} \quad (13)$$

where $\zeta[\alpha]$ is the open-loop normalized variance from equation 15 in the Appendix.

In[309]:= **Table3**

v (m/s)	T (ms)	$\tau_c=0.T$	$\tau_c=0.5T$	$\tau_c=1.T$	$\tau_c=2.T$
9	0.5	26.2898	31.8299	37.1939	47.467
9	1.25	56.4163	68.3048	79.8157	101.861
19	0.5	49.002	59.3281	69.3262	88.4743
19	1.25	105.155	127.314	148.77	189.86

Out[309]=

Table 3. Values of open-loop control bandwidth error σ , in nanometers rms, for the cases studied.

For closed-loop control we use

$$\sigma[v_-, T_-, \alpha_-, \gamma_-] := \left(\frac{500}{2\pi}\right) \sqrt{\zeta[\alpha, \gamma] \left(\frac{v T}{r_0}\right)^{5/3}} \quad (14)$$

where $\zeta[\alpha, \gamma]$ is the closed-loop normalized variance from equation 16 in the Appendix, and use the value of feedback gain, γ , that minimizes the residual in each delay case. From the Appendix, these values are $\gamma = 0.6, 0.5, 0.4,$ and 0.3 respectively for compute delays of 0, 1/2, 1, and 2 time samples, respectively.

In[318]:= **Table4**

v (m/s)	T (ms)	$\tau_c=0.T$	$\tau_c=0.5T$	$\tau_c=1.T$	$\tau_c=2.T$
9	0.5	26.6718	33.2414	40.1813	53.2174
9	1.25	57.236	71.334	86.2265	114.201
19	0.5	49.714	61.9592	74.8945	99.1926
19	1.25	106.683	132.96	160.719	212.861

Out[318]=

Table 4. Values of closed-loop control bandwidth error, in nanometers rms, for the cases studied.

■ References

1. Greenwood, D. P., "Bandwidth Specification for Adaptive Optics Systems," JOSA-A, 67, 3, 1977, pp. 390-392.
2. Chanan, G., et. al., "Adaptive Optics for Keck Observatory," Keck Observatory Report No. 208, 1996.
3. KAON 644, "Build-to-Cost Architecture Performance Analysis," Appendix.

■ Appendix: Rejection performance of discrete-time control laws

In this section we calculate ζ for the discrete-time control laws. As mentioned in the main text, ζ is considerably higher in the case of a real system with delays than it is in the simplified models.

■ Open loop transfer function curves

The following are curves of the open loop transfer function (equation 3) and the corresponding residual power spectrum.

In[264]:= **FigureA1**

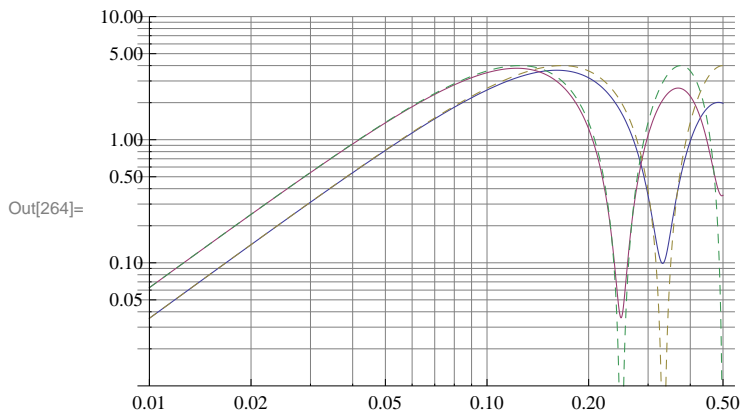


Figure A1. Open loop transfer functions for 1 and 2 sample-time compute delays (increasing crossover frequency with decreasing compute delay). The dashed curves represent the "average age of data" approximation where we substitute the WFS stare and DM hold transfer functions each with 1/2 sample time delays.

In[265]:= **FigureA2**

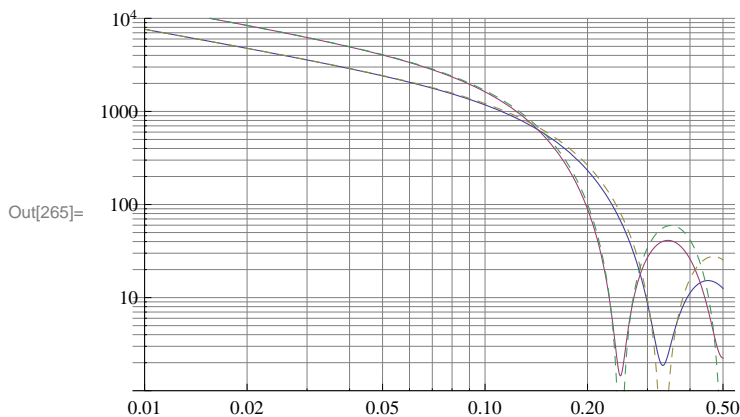


Figure A2. Open loop residual spectra for 1 and 2 sample-time compute delays (decreasing residual with decreasing compute delay). The dashed curves represent the "average age of data" approximation where we substitute the WFS stare and DM hold transfer functions each with 1/2 sample time delays.

The integrated residual spectra is evaluated for the case of the compute delay, τ_c equals 0, 1/2, 1, and 2 time samples and the camera readout delay equals 1 time sample to calculate the respective normalized variances:

OLNV

In[5]:= $\zeta[\alpha_] :=$

$$0.0770491 \times 2 \left(\text{NIntegrate} \left[\left\| 1 - e^{-i 2 \pi \alpha f} \left(\frac{1 - e^{-i 2 \pi f}}{-i 2 \pi f} \right)^2 \right\|^2 f^{-8/3}, \{f, 10^{-6}, 1/2\} \right] + 12 \pi^2 (1 + \alpha)^2 f_1^{1/3} /. f_1 \rightarrow 10^{-6} \right) // \text{Re} \quad (15)$$

where α is the total delay including readout delay and compute delay, in units of sample period, T.

The following asymptotic formula is used to help compute the portion of the integral near $f = 0$:

$$\text{Series}\left[\left(1 - e^{-i 2 \pi \alpha f} \left(\frac{1 - e^{-i 2 \pi f}}{-i 2 \pi f}\right)^2\right) \left(1 - e^{i 2 \pi \alpha f} \left(\frac{1 - e^{i 2 \pi f}}{i 2 \pi f}\right)^2\right) f^{-8/3}, \{f, 0, 3\}\right]$$

$$\frac{4 \pi^2 (1 + \alpha)^2}{f^{2/3}} - \frac{1}{9} (\pi^4 (23 + 72 \alpha + 84 \alpha^2 + 48 \alpha^3 + 12 \alpha^4)) f^{4/3} + O[f]^{10/3}$$

$$\text{Integrate}\left[\frac{4 \pi^2 (1 + \alpha)^2}{f^{2/3}}, \{f, 0, f_1\}\right]$$

$$12 \pi^2 (1 + \alpha)^2 f_1^{1/3}$$

■ Closed loop transfer function curves

The following are curves of the closed loop transfer function (equation 4) and the corresponding residual power spectrum.

In[258]:= **FigureA3**

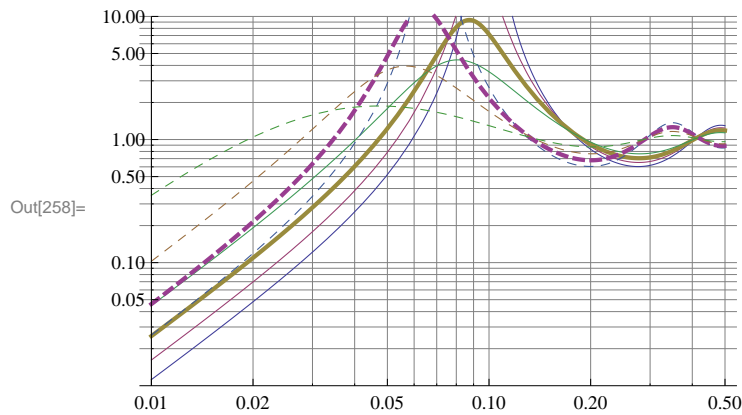


Figure A3. Closed loop transfer functions for various feedback gains (increasing crossover and resonant peak with increasing gain). The solid lines are for one sample time compute delay; dashed lines are two sample times of compute delay. Thick lines indicate optimal total-power-rejection curves for a Kolmogorov disturbance input spectrum.

In[259]:= **FigureA4**

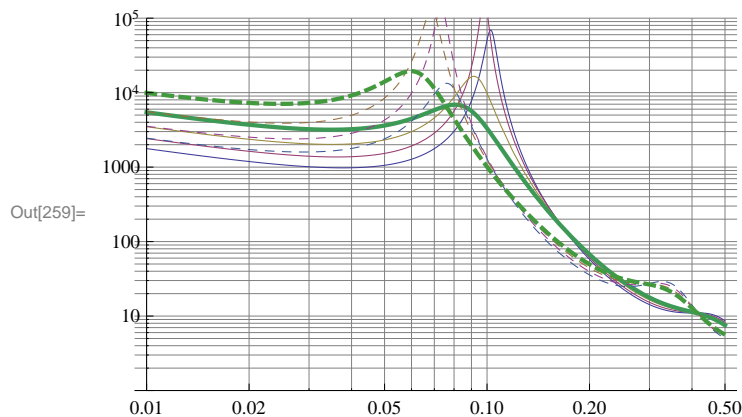


Figure A4. Closed loop residual spectra for various feedback gains (increasing crossover and resonant peak with increasing gain). The solid lines are for one sample time compute delay; dashed lines are two sample times of compute delay. Thick lines indicate the least-total-integrated power curves.

The integrated closed loop residual spectra is evaluated for the case of the compute delay, τ_c equals 0, 1/2, 1, and 2 time samples and the camera readout delay equals 1 time sample to calculate the respective normalized variances. In this case we must find the feedback gain, γ , that minimizes the residual within a range where the control loop is stable.

CLNV

$$\ln[11]:= \zeta[\alpha_-, \gamma_-] := 0.0770491 \times 2 \left(\text{NIntegrate} \left[\left\| \frac{1}{1 + \frac{\gamma}{1 - e^{-i 2 \pi f}} e^{-i 2 \pi \alpha f} \left(\frac{1 - e^{-i 2 \pi f}}{-i 2 \pi f} \right)^2} \right\|^2 f^{-8/3}, \{f, 10^{-6}, 1/2\} \right] + \frac{12 \pi^2 f_1^{1/3}}{\gamma^2} /. f_1 \rightarrow 10^{-6} \right] // \text{Re} \quad (16)$$

In[263]:= **TableA1**

ζ_{CL}	$\tau_c=0. T$	$\tau_c=0.5 T$	$\tau_c=1. T$	$\tau_c=2. T$
$\gamma=0.6$	43.1888	70.0042	268.782	73.6983
$\gamma=0.5$	50.3684	67.0849	108.9	238.783
$\gamma=0.4$	64.7406	77.0322	98.0197	279.958
$\gamma=0.3$	94.6965	104.892	119.002	171.938
$\gamma=0.2$	171.445	181.021	192.586	224.203
$\gamma=0.1$	508.411	519.548	531.724	559.595
$\gamma=0.01$	22427.3	22465.9	22505.	22584.2

Out[263]=

Table A1. Normalized residual variance for a closed-loop discrete time control law with various feedback gains, γ , for various cases of compute-time delay, τ_c .

The integration again required an asymptotic approximation near $f = 0$:

$$\text{Series} \left[\left(\frac{1}{1 + \frac{\gamma}{1 - e^{-i 2 \pi f}} e^{-i 2 \pi \alpha f} \left(\frac{1 - e^{-i 2 \pi f}}{-i 2 \pi f} \right)^2} \right) \left(\frac{1}{1 + \frac{\gamma}{1 - e^{i 2 \pi f}} e^{i 2 \pi \alpha f} \left(\frac{1 - e^{i 2 \pi f}}{i 2 \pi f} \right)^2} \right) f^{-8/3}, \{f, 0, 3\} \right]$$

$$\frac{4 \pi^2}{\gamma^2 f^{2/3}} + \frac{4 (-12 \pi^4 + 12 \pi^4 \gamma + 24 \pi^4 \alpha \gamma + \pi^4 \gamma^2) f^{4/3}}{3 \gamma^4} + O[f]^{10/3}$$

$$\text{Integrate} \left[\frac{4 \pi^2}{\gamma^2 f^{2/3}}, \{f, 0, f_1\} \right]$$

$$\frac{12 \pi^2 f_1^{1/3}}{\gamma^2}$$